



SPE 96375

Analysis of the ensemble Kalman filter for estimation of permeability and porosity in reservoir models

Rolf J. Lorentzen, Geir Nævdal, SPE, Brice Vallès, Aina M. Berg, SPE, Alv-Arne Grimstad, RF-Rogaland Research

Copyright 2005, Society of Petroleum Engineers

This paper was prepared for presentation at the 2005 SPE Annual Technical Conference and Exhibition held in Dallas, Texas, U.S.A., 9 - 12 October 2005.

This paper was selected for presentation by an SPE Program Committee following review of information contained in a proposal submitted by the author(s). Contents of the paper, as presented, have not been reviewed by the Society of Petroleum Engineers and are subject to correction by the author(s). The material, as presented, does not necessarily reflect any position of the Society of Petroleum Engineers, its officers, or members. Papers presented at SPE meetings are subject to publication review by Editorial Committees of the Society of Petroleum Engineers. Electronic reproduction, distribution, or storage of any part of this paper for commercial purposes without the written consent of the Society of Petroleum Engineers is prohibited. Permission to reproduce in print is restricted to a proposal of not more than 300 words; illustrations may not be copied. The proposal must contain conspicuous acknowledgment of where and by whom the paper was presented. Write Librarian, SPE, P.O. Box 833836, Richardson, TX 75083-3836, U.S.A., fax 01-972-952-9435.

Abstract

It has lately been reported several successful applications where the ensemble Kalman filter has been used to estimate reservoir properties such as permeability and porosity. However, a thorough investigation of robustness and performance is still missing for this approach. In this paper we aim at filling this gap by studying the robustness of the methodology. One aspect which is investigated is how the filter depends on the initial ensemble. As the initial ensemble is created in a stochastic way, one can not be certain that the results obtained from one run represent the filter performance. Another aspect of interest is how prior information can be used to obtain best possible initial fields. The influence of geostatistical information on the estimated solutions is studied. In addition, the quality of the estimated fields is investigated by evaluating if the estimated static fields are reasonable when treated as the solution of the history matching problem.

The estimation technique has been applied to the widely used PUNQ-S3 reservoir model, which is a small size synthetic 3-D reservoir engineering model. Both permeability and porosity are tuned, and measurements con-

sist of well bottom-hole pressures, water cuts and gas-oil ratios. The initial fields are conditioned on the porosities in the gridblocks where the wells are located. By using a synthetic reservoir model it is possible to calculate the uncertainty of forecasts, and compare this with the true solution.

Introduction

The ensemble Kalman filter¹ has recently gained popularity as a method for history matching of reservoir models^{2,3,4,5,6,7,8}. These studies show that the ensemble Kalman filter is a promising alternative to other history matching methods for estimating permeability and porosity. One advantage of the ensemble Kalman filter compared to most of the traditional methods is that it generates a set of updated reservoir models representing the uncertainty in the model. The number of reservoir simulations required is equal to the number of models generated.

The ensemble Kalman filter is a Bayesian approach and is initialized by generating permeability and porosity fields using a priori geostatistical assumptions. The production data are incorporated sequentially in time, and the permeability and porosity fields are updated as new production data are introduced. In addition to the static fields (porosity and permeability), dynamic fields such as the reservoir pressure and saturations are updated too. In particular this means that the method is suitable for online updating of the model.

The estimated fields depend on the initial ensemble which is generated stochastically. In a previous study⁷ it was shown that to get a reasonable estimate of the uncertainty of the model parameters a relatively large ensemble was required. In other studies between 40 and 100 ensemble members have been used^{3,4,5}, and reasonable performance of forecasts has been obtained. However, it has not been investigated to which degree the results depended

on the initial ensemble, as the results have been presented using a single ensemble. Here we will perform a more thorough study of this by comparing results obtained using 10 different initial ensembles of size 100 generated from the same distribution.

We will both evaluate the total cumulative oil production forecasted by the filter, and also evaluate if the estimated static fields are reasonable when treated as the solution of the history matching problem.

As the history matching problem is ill-posed one cannot expect to match the true fields, but one would expect that the estimated fields should be able to reconcile the observations that are used when running the filter. This has been tested for the mean of the ensemble as well as for a single ensemble member. We will consider how the results depend on the a priori geostatistical assumptions, as we have run the same example using two different a priori geostatistical assumptions.

The ensemble Kalman filter is appropriately designed to get production forecasts with uncertainty. A range of forecasts can be generated by running one forecast from each of the updated ensemble members. When the production data is assimilated using the ensemble Kalman filter both dynamic variables (pressure and saturations) and the porosity and permeability is updated. In the updating of the dynamic fields, nothing is imposed to enforce the updated variables to be consistent with reservoir equations, and it is therefore interesting to compare forecasts based on the last updated ensemble, with forecasts obtained by rerunning the complete simulation from time zero using the estimated permeability and porosity fields contained in the last ensemble. An alternative approach of the ensemble Kalman filter which aims at getting dynamic fields that are always consistent is suggested by Wen and Chen⁷.

The reservoir model we are using is the well known PUNQ-S3 case, a synthetic model that has been used in several studies to compare the performance of different history matching techniques^{9,10}. Recently, two studies using the ensemble Kalman filter^{4,5} have been added. We have tested the effect of using two different a priori geostatistical assumptions as input to the ensemble Kalman filter to match the production data. We will study how the results vary due to the randomness that is included in using a stochastic approach by running 10 runs. These runs are identical except for the randomness introduced by using a stochastic approach.

Use of the ensemble Kalman filter for estimation of reservoir parameters

The ensemble Kalman filter was developed for estimation of dynamic state variables in large scale non-linear models. It was introduced as an alternative to the extended Kalman filter¹¹. With the ensemble Kalman filter one does not have the same shortcomings as with the extended Kalman filter:

severe computational burden for large scale models and significant linearization errors for strongly nonlinear models. The ensemble Kalman filter is a Monte Carlo approach where an ensemble of model states is used to approximate the necessary covariance matrices. This implies that no linearization of the model function is necessary. In addition, as the number of ensemble members (N) increases, the error in the corresponding covariance matrix decreases as $1/\sqrt{N}$.¹

The (ensemble) Kalman filter was originally developed to update only dynamical state variables. To include estimation of static parameters the state vector is extended¹², and for the system it becomes

$$\mathbf{U} = [\mathbf{V} \mathbf{P} \mathbf{D}]^T,$$

where \mathbf{V} defines the dynamic state variables, \mathbf{P} the model parameters and \mathbf{D} represents measured production data. In this paper the state variables (\mathbf{V}) consist of pressures, water and gas saturations, and solution gas/oil ratios for each grid block in the numerical solution scheme. The model parameters (\mathbf{P}) are porosity and horizontal and vertical (logarithmic) permeability, also defined for each grid block. Measured production data (\mathbf{D}) consist of bottom hole pressures, gas-oil ratios, and water cuts for each well in the reservoir.

The initial ensemble \mathbf{U}^0 is constructed as Gaussian Random Fields (GRFs), and depends upon geostatistical assumptions about the reservoir. A more detailed description of the procedure used can be found in the ‘‘Example’’ section herein. We note here that the permeability and porosity fields are generated stochastically based on the a priori geostatistical assumptions, whereas we ignore the uncertainty in the initial state of the dynamic variables. Initially, the dynamic state variables are defined by an equilibrium condition, which is equal to the equilibrium state of the ‘‘true’’ model.

One iteration of the ensemble Kalman filter consists of two steps, a forecast step (giving \mathbf{U}_f) and an analysis step (giving \mathbf{U}_a). The forecast step is calculated by using the model function (in our case the reservoir simulator) to propagate the state vectors (ensemble) from timestep $n-1$ to timestep n

$$\mathbf{U}_f^{n,i} = \mathbf{f}(\mathbf{U}_a^{n-1,i}),$$

where i runs from 1 to the number of ensemble members (N).

In the analysis step, the forecast state vectors \mathbf{U}_f^n are updated by taking into account the mismatch between measurements and the corresponding predictions from the ensemble members. The state vectors are related to the measured variables through the following equation

$$\mathbf{D} = \mathbf{H}\mathbf{U},$$

where \mathbf{H} is a matrix that selects calculated measurements from the state vector. Note here that it is necessary to

include the measured variables explicitly in the state vector, in order to get a linear relationship between \mathbf{U} and \mathbf{D} . Further we assume that the true observation vector at time n is given by \mathbf{D}_o^n . It can be shown¹³ that to get the correct error propagation during the analysis step, it is necessary to construct an ensemble of observation vectors according to

$$\mathbf{D}_o^{n,i} = \mathbf{D}_o^n + \epsilon_o^{n,i},$$

where each $\epsilon_o^{n,i}$ is drawn from a normal distribution with zero mean and covariance matrix \mathbf{R}^n . The analyzed states are now computed as

$$\mathbf{U}_a^{n,i} = \mathbf{U}_f^{n,i} + \mathbf{K}^n(\mathbf{D}_o^{n,i} - \mathbf{H}\mathbf{U}_f^{n,i}),$$

where \mathbf{K}^n is called the Kalman gain matrix and is given by

$$\mathbf{K}^n = \mathbf{P}_f^n \mathbf{H}^T (\mathbf{H} \mathbf{P}_f^n \mathbf{H}^T + \mathbf{R}^n)^{-1}.$$

The matrix \mathbf{P}_f^n is an approximation to the model error covariance matrix, and can be written as

$$\mathbf{P}_f^n = \mathbf{L}_f^n (\mathbf{L}_f^n)^T,$$

where \mathbf{L}_f^n is given by

$$\mathbf{L}_f^n = \frac{1}{\sqrt{N-1}} \left[(\mathbf{U}_f^{n,1} - \widehat{\mathbf{U}}_f^n) \dots (\mathbf{U}_f^{n,N} - \widehat{\mathbf{U}}_f^n) \right].$$

Here $\widehat{\cdot}$ represents ensemble mean. Assuming normal distributions, the mean of the analyzed ensemble

$$\widehat{\mathbf{U}}_a^n = \frac{1}{N} \sum_{i=1}^N \mathbf{U}_a^{n,i},$$

is the best estimate for the model state at timestep n .

Measures of filter performance The filter performance is evaluated by using estimated parameter fields in history matching exercises. Estimated permeability and porosity from a given timestep are used as initial values for the simulator, together with dynamic variables in equilibrium state. Synthetic measurements are generated by running the simulator through the complete history matching period. The history match measure is given as

$$\text{HM}(k) = \sqrt{\frac{1}{M} \sum_{n=1}^{M_T} \sum_{j=1}^{M_n} \left[\frac{(\mathbf{D}_o^n(j) - \mathbf{D}_{h,k}^n(j))^2}{\sigma_{n,j}^2} \right]}, \quad (1)$$

where M_T is the number of assimilation steps, i.e. steps where the state vector is updated, M_n is the number of measurements at step n , M is the total number of measurements, and $\sigma_{n,j}$ is the standard deviation of the measurement error. The vectors $\mathbf{D}_{h,k}^n$ are the calculated (history matched) measurements when fixed estimated static parameters estimated at timestep k are used. The subscript h is added to distinguish these values from the Kalman filter output.

Example: PUNQ-S3

The PUNQ-S3 is a small-size synthetic 3-D reservoir engineering model. The model is based on a real field that was managed by Elf Exploration Production. A full description can be found at the PUNQ-S3 website¹⁴ and in Floris *et. al.*⁹ Here we include a short description. The PUNQ-S3 model was given to several oil companies and universities who were asked to predict the total cumulative oil production based on noisy measurements, field operation history and geostatistical information for the true permeability and porosity fields. The participants were asked to give three estimates, P10, P50 and P90, representing the 10 %, 50 %, and 90 % quantiles of the simulated results.

Production and measurements The reservoir consists of $19 \times 28 \times 5$ gridblocks, where 1761 are active. The gridblocks have equal 180 meter sides in x- and y-directions. The heights of the gridblocks are varying. Fig. 1 shows the top layer of the reservoir, including six production wells (black circles). The reservoir is bounded by a sealing fault in the east and south and is bounded by a strong aquifer in the west and north. This aquifer ensures high reservoir pressure and makes injection wells redundant. The red zone in the figure indicates a gas cap.

The production schedule is divided into two sections. The first section lasts 8 years and is considered as a history matching phase. This section consists of one year of extended well testing, a 3 year shut-in period and 4 years of production. During this period, the wells are operated on target oil rates. When running the ensemble Kalman filter we run the first 8 years in a history matching mode, which means that the wells are steered according to the observed values generated by running the simulator using the “true” permeability and porosity fields. The rates used are those specified in the description of the PUNQ-S3 example.¹⁴

The second section consists of 8.5 years of production. A shut-in test is performed for two weeks each year for all wells (during this phase). The wells are controlled using a target oil rate of 150 scm/day. If the bottom hole pressure goes below 120 bar, this value is used as a target pressure. Further, if the gas/oil ratio is greater than 200 scm/scm, the oil rate in the wells is reduced by a factor of 0.75.

Measurements from all six wells were used during the assimilation period. This include bottom hole pressures, gas-oil ratios, and water cuts. The measurement uncertainties for these measurements are collected from the PUNQ-S3 website¹⁴. The shut-in pressure has a noise level of 1 bar whereas flowing pressure has a noise level of 3 bar. The gas-oil ratios have a measurement uncertainty of 10 % before gas breakthrough and 25 % after gas breakthrough. The water cut has 2 % uncertainty before water breakthrough and 5 % after. We have assumed that the measurements noise is uncorrelated, and we have used the same noise level generating the observations as when run-

ning the filter.

Initial ensemble The initial ensemble is constructed based on prior geostatistical information. In order to investigate the importance of this information, we have constructed the initial ensembles for the investigations in this paper by two different procedures.

The first procedure is similar to the one described on the PUNQ-S3 website¹⁴. It can be summarized as follows: First the function *sgsim* from the GSLIB¹⁵ software library is used to generate a normalized GRF for the porosity, conditioned on well data. Further, collocated co-simulation, *sgcosim*, is used to generate normalized GRFs for horizontal and vertical permeabilities conditioned on well data and correlated to the porosity with a correlation coefficient of 0.8. The procedure depends on geostatistical parameters describing principal directions, correlation lengths, and anisotropy ratios. For this first procedure we use values for these parameters taken from the description of the generation of the true case in¹⁴.

The second procedure for generation of initial ensembles is as described in the paper by Barker *et. al.*¹⁰ Also in this procedure the porosity is generated as a GRF conditioned on well data, but with geostatistical parameters which differ considerably from the true case. Deterministic relationships are used to calculate horizontal and vertical permeability. The equations are

$$\log(k_h) = 9.02\phi + 0.77, \quad k_v = 0.31k_h + 3.12, \quad (2)$$

where k_h is the horizontal permeability, ϕ is the porosity and k_v is the vertical permeability. The relationship between the porosity and the permeabilities given in (2) is only used when generating the initial ensemble, and will generally not be preserved in the ensemble Kalman filter run.

The fields are in both cases transformed to meet given means and standard deviations and also to lie within given physical ranges.

The well data used for conditioning the porosity and permeability fields are constructed in the following manner: The normalized well data values found on the PUNQ-S3 website¹⁴ are transformed to real values, for porosity and permeabilities, using the relevant geostatistical parameters for the two procedures described above, and used as “measured” values. The conditioning data for each ensemble member is obtained by adding Gaussian noise with a standard deviation of 15 % to the measured values. Each ensemble member is conditioned to a separate set of “noisy” well data in order to get variation in the ensemble also at the position of the wells.

We have chosen to use 100 ensemble members. An ensemble size of this order has been found to be sufficient for similar applications and other large scale models¹⁶.

In the following, *Case A* refers to the case where a pro-

cedure similar to the one found on the PUNQ-S3 website¹⁴ is used to generate the initial porosity and permeability fields. In *Case B*, the procedure described by Barker *et. al.*¹⁰ is used to generate the initial fields. In both Case A and Case B we have performed 10 runs with different initial ensembles.

Results In the following we present several production forecasts. Each forecast figure shows results when ten different initial ensembles are used. This is done in order to investigate the robustness, as the results for each different initial ensemble should be comparable. Further, for each run we show the 10 %, 50 %, and 90 % quantiles for the forecast uncertainty function (P10, P50, and P90). We also show the forecast resulting from using the mean of the ensemble (P_m), and the forecast resulting from using a single ensemble member (P_f). Note that the last two measures are cheaper to obtain in the sense that it is not necessary to calculate forecasts for all the ensemble members. We have chosen to also run forecasts for a single ensemble member (arbitrarily chosen as the first member), since the mean of the ensemble could possibly contain features that are not present for individual ensemble members. We also show the true cumulative oil production as a reference. All forecasts are evaluated at 6025 days (16.5 years).

Three different types of forecasts are shown. The first is the results when the initial ensemble is used to calculate the forecasts. In this case the forecast is run for 16.5 years. The results is presented in Figure 2.

The second type of forecasts are generated by using the fields (static and dynamic) estimated by the Kalman filter at 2936 days (8 years) as the initial state. This is referred to as *Kalman filter forecasts*, and the results are shown in Figure 3.

The third type of forecasts are generated by using the estimated static variables at 2936 days in simulations starting from time zero. That is, the initial equilibrium for the dynamic variables is used as starting point, but in this case the permeability and porosity fields are tuned to include the information provided by the production data. This is referred to as *history match forecasts*. The results are shown in Figure 4.

The results presented in Figure 2–4 can be compared to the results presented in other papers^{5,9,10} studying this example, but note that there are some deviations in the way that the examples are run in the different studies.

In order to make a thorough investigation of the results, we have calculated statistics for the results shown on the figures. These are given in Table 1. Here the first column shows the different cases, where “Ini.” is the case where the initial ensemble is used to generate the forecasts, “KF” is the Kalman filter forecasts and “HM” is the history match forecasts. The other columns show mean values (μ) and standard deviations (σ) for the different forecasts

measures.

From Figure 2–4 and Table 1 some conclusions can be drawn. There is a significant improvement in the quality of the forecasts of cumulative oil production after assimilation of production data. In both cases P50, P_m and P_f are significantly improved, and the spread (measured as $P_{90} - P_{10}$) is reduced. In neither case are there any significant differences between the Kalman filter and history match forecasts, except for P_m where the Kalman filter forecasts are better than the history match forecasts. It has been shown earlier that the forecasts of total cumulative oil production improves when the ensemble Kalman filter is used to assimilate production data for the PUNQ-S3 model^{4,5}, but these papers did not consider the robustness of the approach as results were only shown for a single initial ensemble.

Figure 2 shows that the initial fields with “correct” geostatistical information give better results. But the difference is not as striking after assimilation of production data (Figure 3). It is not yet fully understood how important a role correct prior geostatistical information has in order to obtain the best possible forecasts.

We also notice that the spread in Case A is slightly less than in Case B before assimilation of production data, but after assimilation of production data the spread in Case A is greater than in Case B.

Ideally, the forecasted values should be from the same distribution independent of the initial ensemble. We have used the Kolmogorov-Smirnov test to compare the cumulative distribution function (cdf) of two samples and tested pairwise for different ensembles of forecasts using the MATLAB™ function *kstest2*¹⁷.

With a significance level of 0.01 we have found that we could not reject the hypothesis that the forecasted values have the same cdf when comparing pairwise all the initial forecasts (cf. Figure 2), for both cases. It is rejected, however, that the forecasted total cumulative oil production from any run from Case A has the same cdf as those from Case B.

In Figure 5 we show the empirical cdfs for the Kalman filter forecasts (cf. Figure 3). We can see that the forecasts obtained after assimilation of production data lead to significantly different empirical cdfs. We find that the cdfs can apparently be grouped, and this is confirmed by using the Kolmogorov-Smirnov test. In Case A there are five groups consisting of Run 2, 4, 6 and 8, Run 3, 9, and 10, and three groups consisting of a single run (1,5 and 7). In Case B the cdfs were divided in three groups. One group consists of Run 1, 4, 5, 6, 7, and 10, one of Run 3, 8 and 9, the last of Run 2.

As noted above the forecasts should come from the same underlying distribution, determined by the prior model and the production data. We have not investigated why this seems not to be the case, but it is tempting to

suspect that it is related to the limited ensemble size. Nor have we investigated if there is any underlying reasons for the grouping or if it is coincidental. The cdfs produced by the history match forecasts are very close to those produced from the Kalman filter forecasts, which means that we can rely on using the Kalman filter forecasts that are obtained using less computation.

In addition to the forecasts we show two figures where the ensemble Kalman filter is used as a history match routine. The calculated measurements are collected and compared to the real measurements according to Eq. 1. This is repeated for each assimilation step, i.e. $HM(k)$ is calculated for each available k . This results in a set of points which are plotted. Note that the history match output is dimensionless. If the mismatch between the observed and simulated values can be explained by measurement errors $HM(k)$ should approach a value of one.

In Figure 6 we plot $HM(k)$ for the mean of the ensemble for all the 20 runs. The curves are split across two subfigures for each case in order to distinguish them. Figure 7 shows the history match curves obtained using a member of the ensemble instead of the mean. We show the result for the first member of the ensemble, since the numbering within the ensemble is random.

In both Figure 6 and 7 we see that the general trend is that the history match is improved. As expected, the mean of the ensemble produces more stable results than using a single ensemble member. In all the cases $HM(k)$ approaches one, which means that the estimated static fields reconcile the observation data. Many of the curves have similar features. They usually start with a large reduction just after the start of the production. Close to the shut-in period many are increasing and then having a large drop just after production is again started after this period of three years. It is not clear what drives this, but a large improvement in the estimates by using only the first production data has also been observed previously³.

Conclusions

We have demonstrated that the ensemble Kalman filter is an algorithm that is well suited for producing forecasts with uncertainty. It is observed that the forecasts are improved after assimilation of production data.

The Kalman filter forecasts and the history match forecasts give very similar results. The Kalman filter forecasts are cheaper to compute. This strengthens the support of using the ensemble Kalman filter approach for this problem, in particular as one objection that has been raised is the problem that the final estimated dynamic fields are not necessarily physically consistent. We have not evaluated if the dynamic and static fields are consistent, but they produce forecast that are very similar to those obtained using the estimated static fields and rerunning the simulator from time zero.

We have shown that the estimated static fields, in particular the mean of the ensemble, provides good solution of the history matching problem as the production data are reconciled using these fields. This holds for both Case A and Case B, showing that good solutions are obtained using different geostatistical assumptions.

Acknowledgments

This research has been supported financially by the Norwegian Research Council, Chevron Texaco, Eni, Norsk Hydro, Statoil ASA and Total E & P.

Nomenclature

\mathbf{U}	=	state vector
\mathbf{V}	=	dynamic state variables
\mathbf{P}	=	static parameters
\mathbf{D}	=	measurements
f	=	model function (reservoir simulator)
ϵ	=	stochastic noise
\mathbf{H}	=	measurement matrix
\mathbf{K}	=	Kalman gain matrix
\mathbf{P}	=	covariance matrix for model uncertainty
\mathbf{R}	=	covariance matrix for measurement error
\mathbf{L}	=	left factor of covariance matrix
N	=	ensemble size
k	=	history match index / permeability
j	=	measurement index
σ^2	=	variance
M_T	=	number of assimilation points
M_n	=	number of measurements at timestep n
M	=	total number of measurements
ϕ	=	porosity
P10	=	10 % quantile
P50	=	50 % quantile
P90	=	90 % quantile
P_m	=	forecast using mean ensemble
P_f	=	forecast using first ensemble

Subscripts

f	=	forecast (a priori)
a	=	analyzed (a posteriori)
m	=	model noise
o	=	observation
t	=	true
h	=	horizontal / history matched
v	=	vertical

Superscripts

T	=	matrix transpose
n	=	timestep index
i	=	ensemble member index

References

1. G. Evensen. The ensemble Kalman filter: Theoretical formulation and practical implementation. *Ocean Dynamics*, 53:343–367, 2003.
2. G. Nævdal, T. Mannseth, and E. H. Vefring. Nearwell reservoir monitoring through ensemble Kalman filter. In *SPE/DOE Improved Oil Recovery Symposium*, Tulsa, Oklahoma, April 2002. SPE75235.
3. G. Nævdal, L. M. Johnsen, S. I. Aanonsen, and E. H. Vefring. Reservoir monitoring and continuous model updating using ensemble Kalman filter. *SPE Journal*, 10(1):66–74, March 2005.
4. Y. Gu and D. S. Oliver. History matching of the PUNQ-S3 reservoir model: Using the ensemble Kalman filter. In *SPE Annual Technical Conference and Exhibition*, Houston, Texas, 26-29 September 2004. SPE90962.
5. G. Gao, M. Zafari, and A. C. Reynolds. Quantifying the uncertainty for the PUNQ-S3 problem in a Bayesian setting with RML and EnKF. In *SPE Reservoir Simulation Symposium*, Houston, Texas, 31 January-2 February 2005. SPE93324.
6. N. Liu and D. S. Oliver. Critical evaluation of the ensemble Kalman filter on history matching of geologic facies. In *SPE Reservoir Simulation Symposium*, Houston, Texas, 31 January-2 February 2005. SPE92867.
7. X.-H. Wen and W. H. Chen. Real-time reservoir model updating using ensemble Kalman filter. In *SPE Reservoir Simulation Symposium*, Houston, Texas, 31 January-2 February 2005. SPE92991.
8. N. Liu and D. S. Oliver. Ensemble Kalman filter for automatic history matching of geologic facies. *Journal of Petroleum Science and Engineering*, 47(3-4):147–161, 2005.
9. F. J. T. Floris, M. D. Bush, M. Cuypers, F. Roggero, and A. R. Syversveen. Methods for quantifying the uncertainty of production forecasts: a comparative study. *Petroleum Geoscience*, 7:87–96, 2001.
10. J. W. Barker, M. Cuypers, and L. Holden. Quantifying uncertainty in production forecasts: Another look at the PUNQ-S3 problem. *SPE Journal*, 6:433–441, 2001.
11. P. S. Maybeck. *Stochastic models, estimation, and control*, volume 1. Academic Press, New York, 1979.
12. R. F. Stengel. *Optimal control and estimation*. Dover publications, inc., New York, 1994.
13. G. Burgers, P. J. van Leeuwen, and G. Evensen. On the analysis scheme in the ensemble Kalman filter. *Monthly Weather Review*, 126:1719–1724, 1998.
14. PUNQ-S3 website: <http://www.nitg.tno.nl/punq/cases/punqs3/index.html>.

15. C. V. Deutsch and A. G. Journel. *GSLIB Geostatistical Software Library and User's Guide*. Applied Geostatistics Series. Oxford University Press, second edition, 1998.
16. P. L. Houtekamer and H. L. Mitchell. Data assimilation using an ensemble Kalman filter technique. *Monthly Weather Review*, 126:796–811, 1998.
17. <http://www.mathworks.com>.

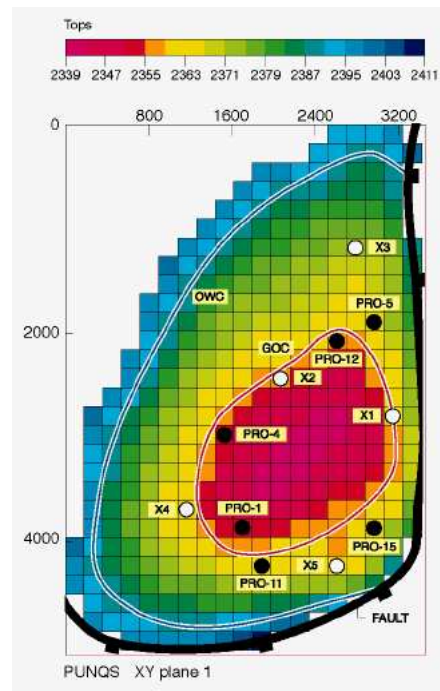
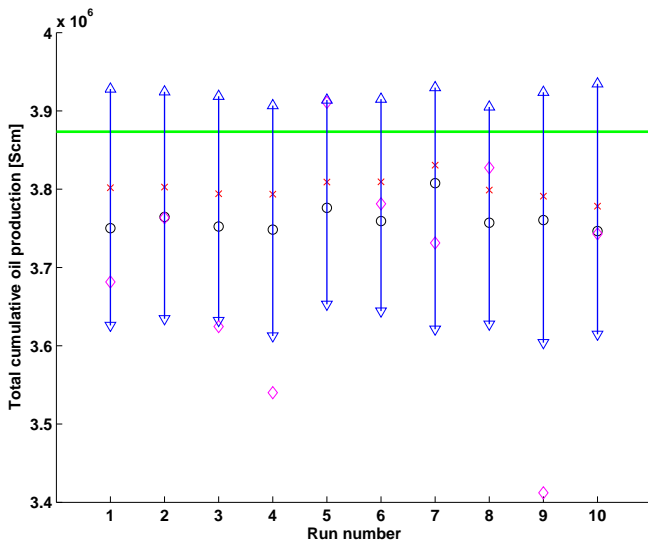


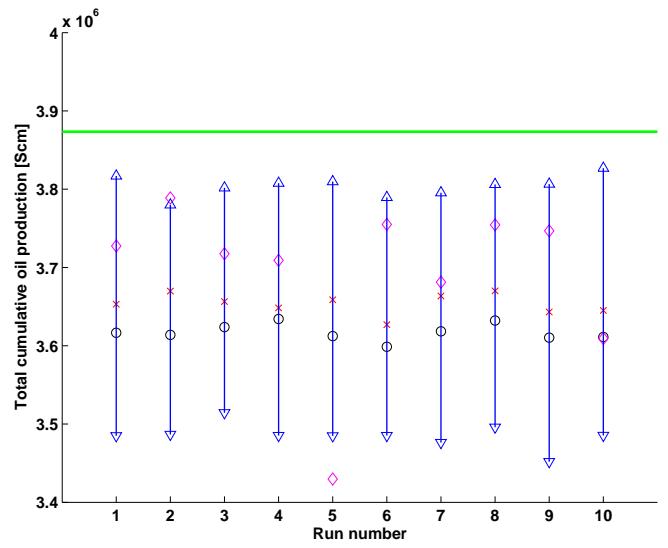
Figure 1: Top layer of PUNQ-S3 reservoir (from the PUNQ-S3 website¹⁴). The black circles show the positions of the wells used in this study.

	$P_{90} - P_{10}$		$ P_m - P_t $		$ P_{50} - P_t $		$ P_f - P_t $	
	$\mu \times 10^4$	$\sigma \times 10^4$						
Ini. - A	29.3	2.00	11.1	1.82	7.24	1.39	17.9	13.4
Ini. - B	31.9	2.10	25.6	1.06	22.0	1.33	18.1	10.4
KF - A	17.0	3.09	4.20	4.51	3.28	3.72	8.78	7.52
KF - B	13.4	1.32	6.05	3.45	5.06	3.14	6.23	4.79
HM - A	17.6	3.63	5.41	5.17	3.36	3.41	9.08	7.23
HM - B	13.2	1.39	7.23	3.06	5.14	2.93	6.40	4.93

Table 1: Statistics for production forecasts. Case A is similar to the original PUNQ-S3 procedure for generating initial fields, and Case B is the procedure described by Barker *et al.*¹⁰

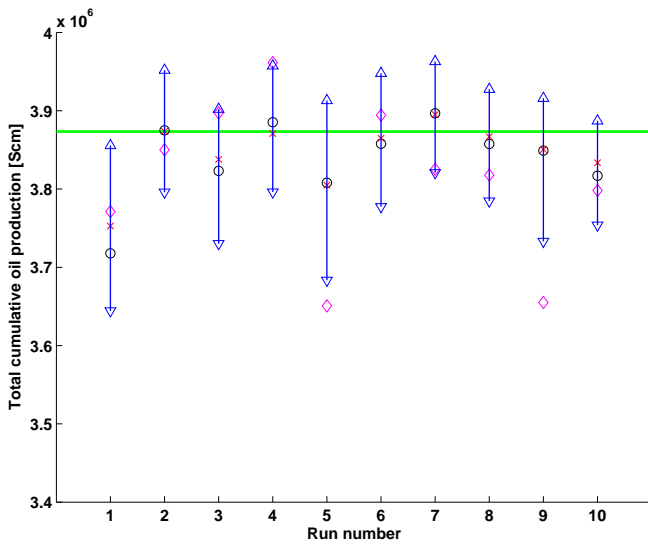


(a) Initial forecast for Case A.

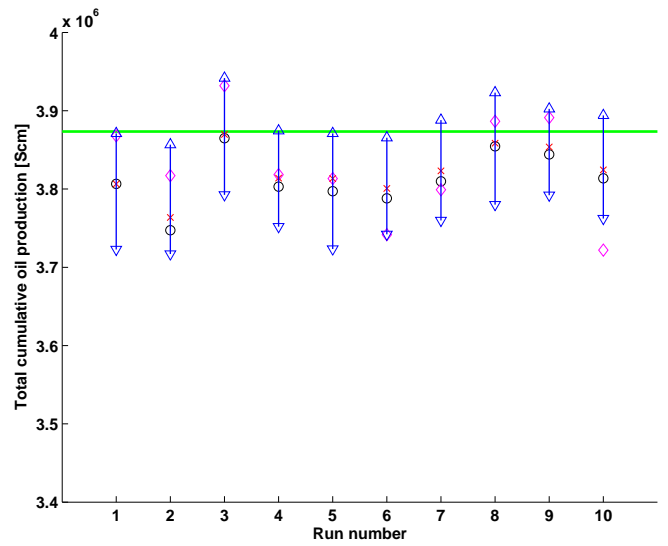


(b) Initial forecast for Case B.

Figure 2: Initial forecasts. The figure shows P10 (∇), P50 (\times), P90 (Δ), P_m (\circ) and P_f (\diamond). The true value is shown as a green line.

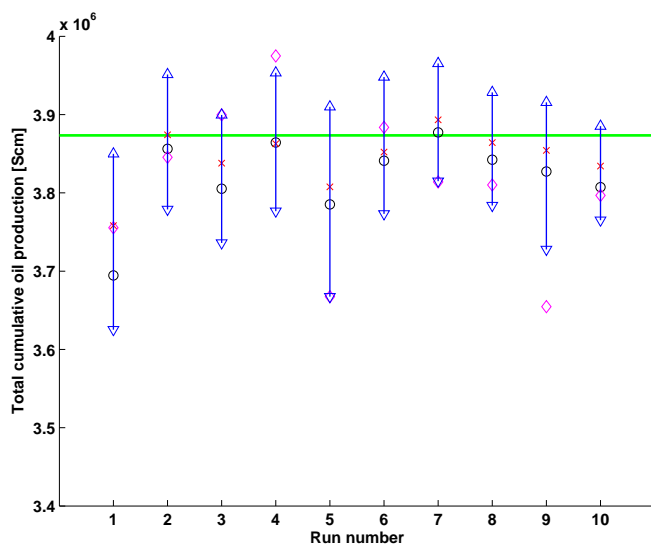


(a) Kalman filter forecast for Case A.

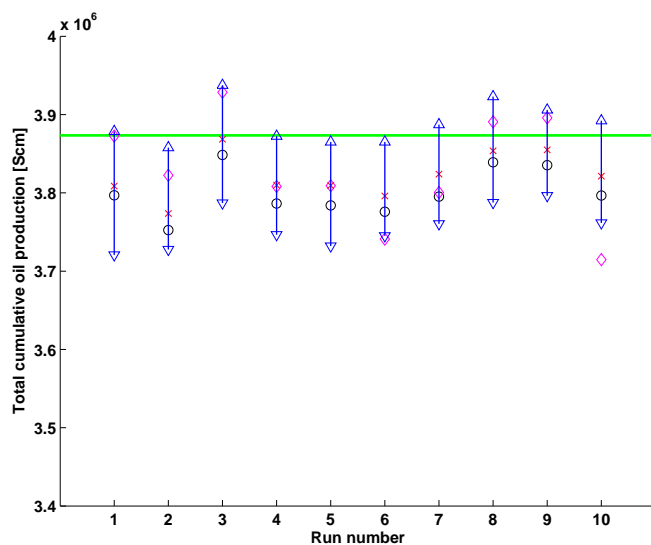


(b) Kalman filter forecast for Case B.

Figure 3: Kalman filter forecasts. The figure shows P10 (∇), P50 (\times), P90 (Δ), P_m (\circ) and P_f (\diamond). The true value is shown as a green line.

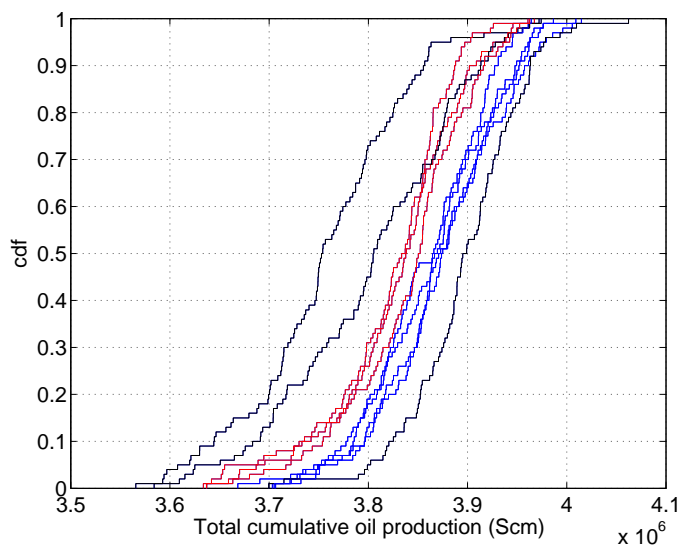


(a) History match forecast for Case A.

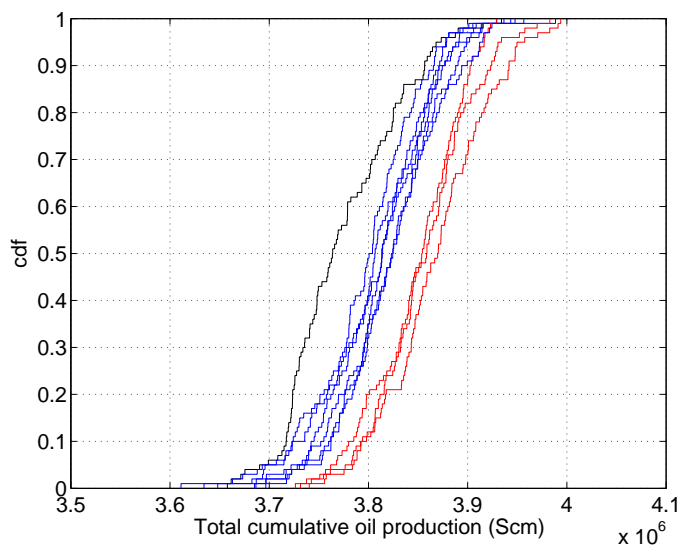


(b) History match forecast for Case B.

Figure 4: History match forecasts. The figure shows P10 (∇), P50 (\times), P90 (Δ), P_m (\circ) and P_f (\diamond). The true value is shown as a green line.



(a) Cumulative distribution function for the Kalman filter forecast for Case A. The cdf for Run 1, 5, and 7 are in black, for Run 2, 4, 6, and 8 are in blue, and for Run 3, 9 and 10 are in red.



(b) Cumulative distribution function for the Kalman filter forecast for Case B. The cdf for Run 2 is in black, for Run 1, 4, 5, 6, 7, and 10 are in blue, and for Run 3, 8 and 9 in red.

Figure 5: Cumulative distribution function for the Kalman filter forecasts.

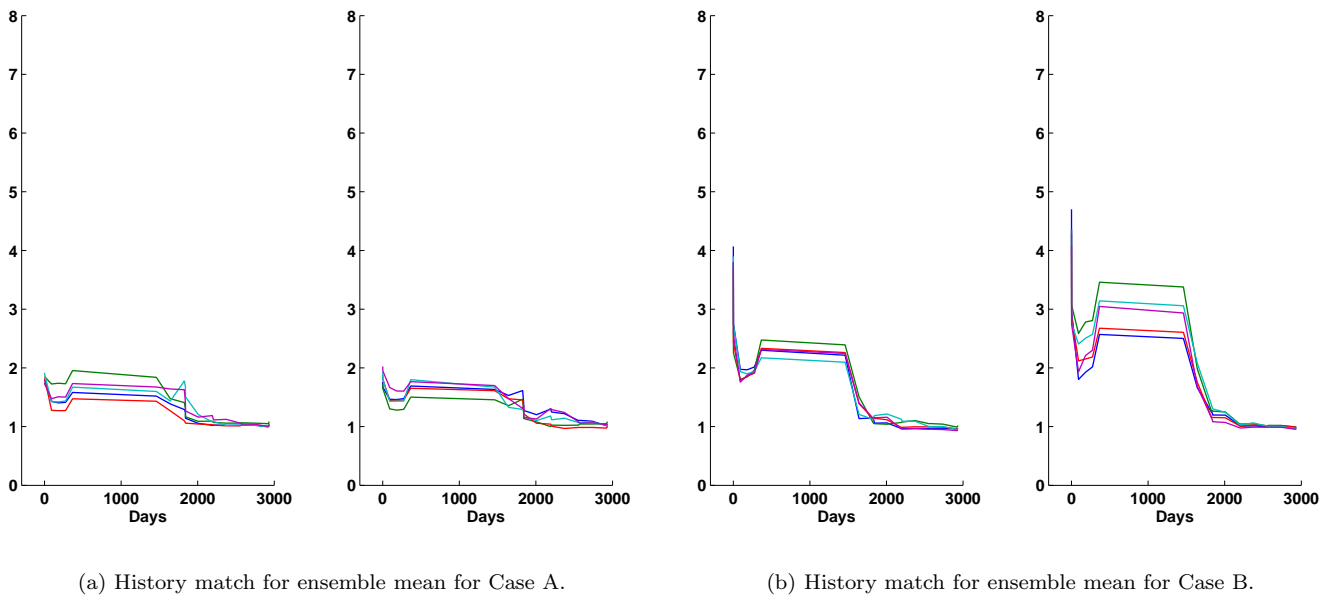


Figure 6: History match for the ensemble mean. The ten curves for each case, split across two sub-figures, represent the runs using different initial ensembles.

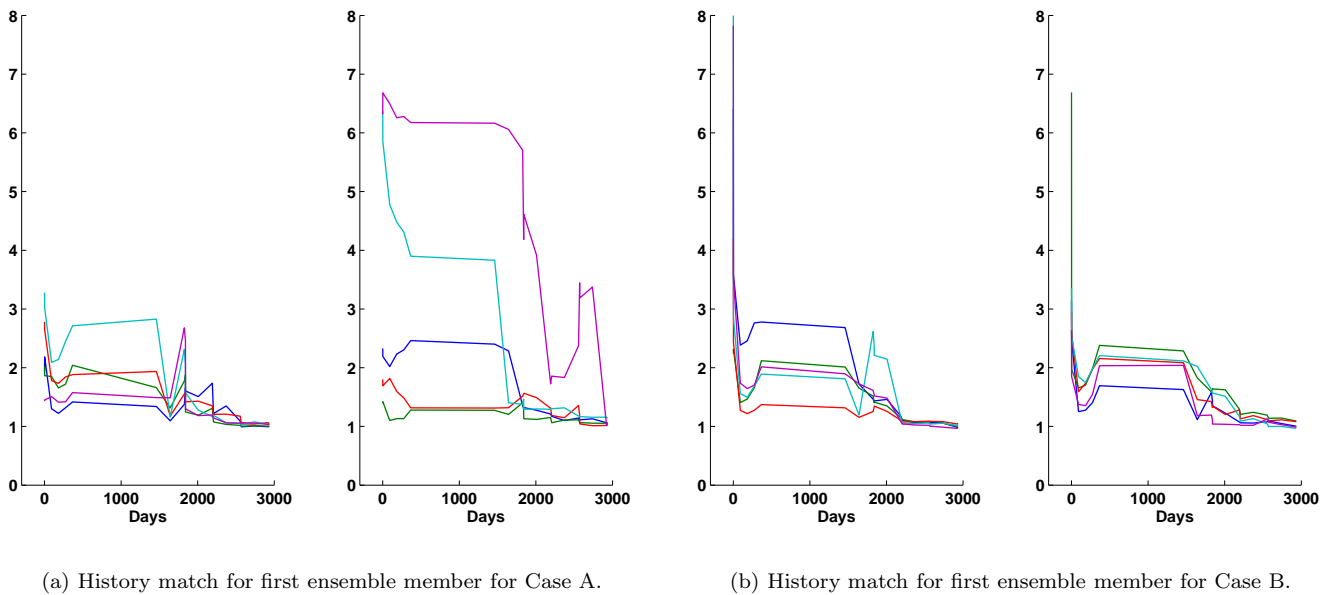


Figure 7: History match for the first ensemble member. The ten curves for each case, split across two sub-figures, represent the runs using different initial ensembles.